Linear
Synchronous
Motors

Gieras | Piech | Tomczuk

Linear Synchronous Motors

CRC Press

K11972

ISBN: 978-1-4398-4221-8
90000
9 781439 842218

www.crcpress.com

CRC Press
Taylor & Francis Group
an **informa** business
www.crcpress.com

6000 Broken Sound Parkway, NW
Suite 300, Boca Raton, FL 33487
711 Third Avenue
New York, NY 10017
2 Park Square, Milton Park
Abingdon, Oxon OX14 4RN, UK

Linear Synchronous Motors

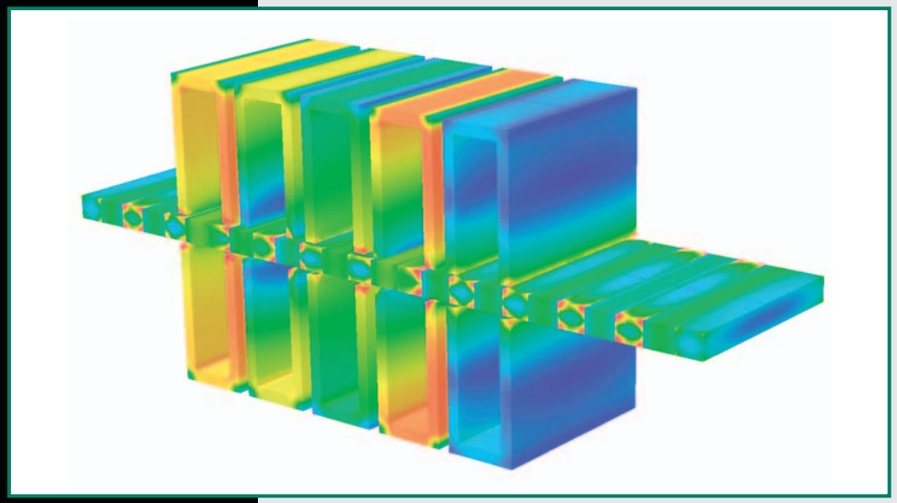

Jacek F. Gieras
Zbigniew J. Piech
Bronisław Tomczuk

CRC Press
Taylor & Francis Group

Jacek F. Gieras

University of Technology and Life Sciences, Bydgoszcz, Poland

Zbigniew J. Piech

Otis Elevator Company, Farmington, CT, U.S.A.

Bronislaw Z. Tomczuk

University of Technology, Opole, Poland

Linear Synchronous Motors

Transportation and Automation Systems

2nd Edition

Taylor & Francis

Contents

Preface to the 2nd Edition

Twelve years have passed since the publication of the first edition of this book in 1999.

The growth in demand for linear motors is principally driven by the replacement of traditional mechanical (ball screws, gear trains, cams), hydraulic, or pneumatic linear motion systems in manufacturing processes, machining, material handling, and positioning with direct electromechanical drives. The linear motor market heavily depends on the semiconductor industry (applications) and permanent magnet industry (linear motors manufacture). A recent market study[1] shows that linear motors have impacted the linear motion market less than expected. The main obstacle that makes companies reluctant to replace mechanical, hydraulic, and pneumatic actuators with linear electric motors is the higher initial cost of installation of direct linear motor drives as compared to traditional mechanical drives.

The North American market for linear motors totaled only US$ 40 million in 1999 and grew by over 20% annually to reach the size of US$ 95 million in 2004. In the same year, the European linear motor market reached the size of US$ 114 million [67]. These numbers do not include special applications and large linear motors (rollercoasters, people movers, military applications). In 2007, the worldwide linear motor component market was estimated at about US$ 230 million, and the worldwide linear motor system market at about US$ 400 million [42]. The worldwide linear motor markets estimated growth between 2007 and 2009 was over 10% for components and over 15% for systems. Linear motors sales fell by close to 50% in 2009 due to global economic recession. The first signs of recovery were visible in the 2nd quarter of 2010. In the future, the main market players will be those manufacturers who can offer complete direct-drive systems.

[1] IMS Research, Wellingborough, UK

All the above numbers are very small in comparison with the world market for standard rotary electric motors. The worldwide market for electric motors grew from US$ 12.5 billion in 2000 to US$ 19.1 billion in 2005 and is predicted to reach US$ 39.1 billion by the year 2015.

In comparison with the 1st edition of this book, the 2nd edition has been thoroughly revised and expanded, Chapter 4, Chapter 5, Appendix D, and List of Patents have been added, and at the end of each chapter, examples of calculations or mathematical models have been added.

The authors hope that the improved and updated new edition of *Linear Synchronous Motors* will find broad readerships including engineers, researchers, scientists, students, and all enthusiasts of linear motors and direct drives.

Prof. Jacek F. Gieras, FIEEE
e-mail: jgieras@ieee.org

Connecticut, June 2011

1

Topologies and Selection

1.1 Definitions, Geometry, and Thrust Generation

Linear electric motors can drive a linear motion load without intermediate gears, screws, or crank shafts. A *linear synchronous motor* (LSM) is a linear motor in which the mechanical motion is in synchronism with the magnetic field, i.e., the mechanical speed is the same as the speed of the traveling magnetic field. The thrust (propulsion force) can be generated as an action of

- traveling magnetic field produced by a polyphase winding and an array of magnetic poles N, S,...,N, S or a variable reluctance ferromagnetic rail (LSMs with a.c. armature windings);
- magnetic field produced by electronically switched d.c. windings and an array of magnetic poles N, S,...,N, S or variable reluctance ferromagnetic rail (linear stepping or switched reluctance motors).

The part producing the traveling magnetic field is called the *armature* or *forcer*. The part that provides the d.c. magnetic flux or variable reluctance is called the *field excitation system* (if the excitation system exists) or *salient-pole rail*, *reaction rail*, or *variable reluctance platen*. The terms *primary* and *secondary* should rather be avoided, as they are only justified for linear induction motors (LIM) [63] or transformers. The operation of an LSM does not depend on, which part is movable and which one is stationary.

Traditionally, a.c. polyphase synchronous motors are motors with d.c. electromagnetic excitation, the propulsion force of which has two components: (1) due to the traveling magnetic field and d.c. current magnetic flux (synchronous component) and (2) due to the traveling magnetic field and variable reluctance in d- and q-axis (reluctance component). Replacement of d.c. electromagnets with permanent magnets (PMs) is common, except for LSMs for magnetically levitated vehicles. PM brushless LSMs can be divided into two groups:

- PM LSMs in which the input current waveforms are sinusoidal and produce a traveling magnetic field;

- PM d.c. linear brushless motors (LBMs) with position feedback, in which the input rectangular or trapezoidal current waveforms are precisely synchronized with the speed and position of the moving part.

Construction of magnetic and electric circuits of LSMs belonging to both groups is the same. LSMs can be designed as flat motors (Fig. 1.1) or tubular motors (Fig. 1.2). In d.c. brushless motors, the information about the position of the moving part is usually provided by an absolute position sensor. This control scheme corresponds to an *electronic commutation*, functionally equivalent to the mechanical commutation in d.c. commutator motors. Therefore, motors with square (trapezoidal) current waveforms are called *d.c. brushless motors*.

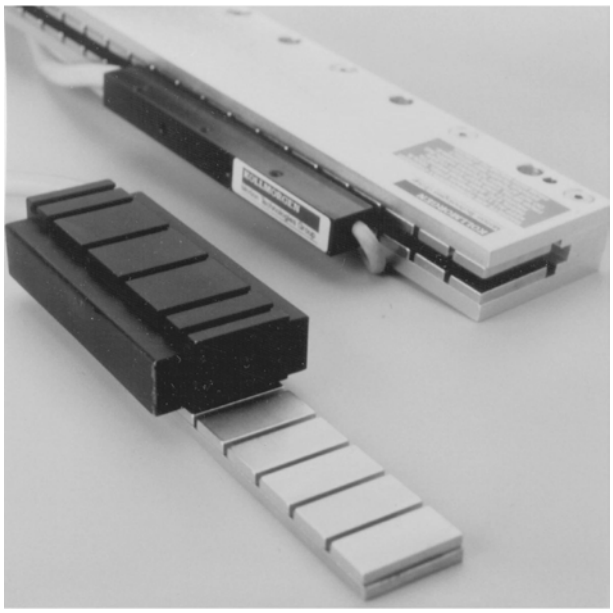

Fig. 1.1. Flat three-phase PM linear motors. Photo courtesy of Kollmorgen, Radford, VA, USA.

Instead of d.c. or PM excitation, the difference between the d- and q-axis reluctances and the traveling magnetic field can generate the reluctance component of the thrust. Such a motor is called the a.c. *variable reluctance* LSM. Different reluctances in the d- and q-axis can be created by making salient ferromagnetic poles using ferromagnetic and nonferromagnetic materials or using anisotropic ferromagnetic materials. The operation of LBMs can be regarded as a special case of the operation of LSMs.

In the case of LSMs operating on the principle of the traveling magnetic field, the speed v of the moving part

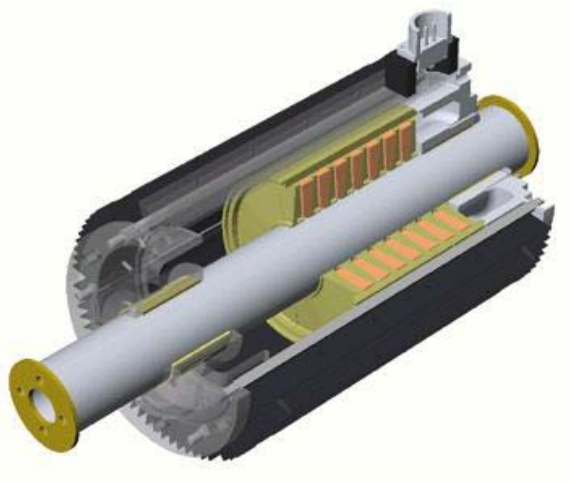

Fig. 1.2. Tubular PM LSM. Moving rod (reaction rail) contains circular PMs [192]
.

$$v = v_s = 2f\tau = \frac{\omega}{\pi}\tau \tag{1.1}$$

is equal to the *synchronous speed* v_s of the traveling magnetic field and depends only on the input frequency f (angular input frequency $\omega = 2\pi f$) and pole pitch τ. It does not depend on the number of poles $2p$.

As for any other linear-motion electric machine, the useful force (thrust) F_x is directly proportional to the output power P_{out} and inversely proportional to the speed $v = v_s$, i.e.,

$$F_x = \frac{P_{out}}{v_s} \tag{1.2}$$

Direct electromechanical drives with LSMs for factory automation systems can achieve speeds exceeding 600 m/min = 36 km/h and acceleration of up to 360 m/s^2 [67]. The thrust density, i.e., thrust per active surface $2p\tau L_i$

$$f_x = \frac{F_x}{2p\tau L_i} \text{ N/m}^2 \tag{1.3}$$

of LSMs is higher than that of LIMs (Fig. 1.3).

The polyphase (usually three-phase) armature winding can be distributed in slots, made in the form of concentrated-parameter coils or made as a coreless (air cored) winding layer. PMs are the most popular field excitation systems for short traveling distances (less than 10 m), e.g., factory transportation or automation systems. A long PM rail would be expensive. Electromagnetic excitation is used in high-speed passenger transportation systems operating

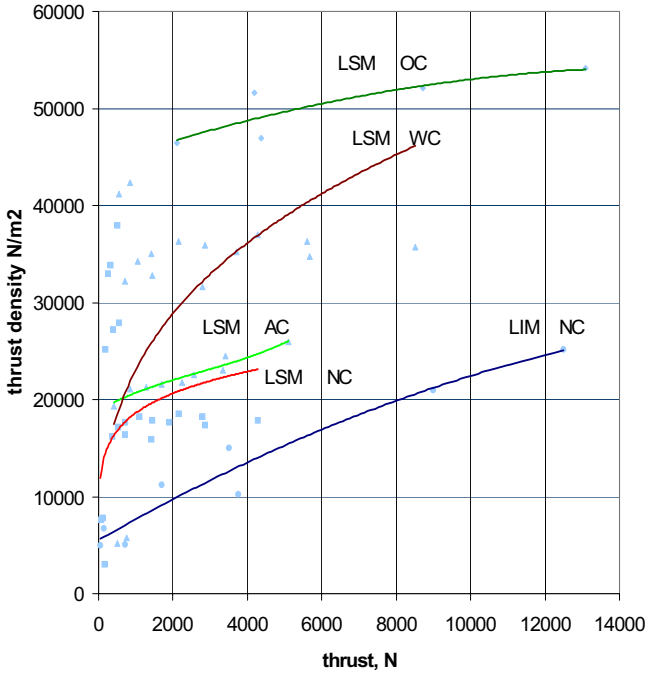

Fig. 1.3. Comparison of thrust density for single-sided LIMs and LSMs: AC — air cooling, NC — natural cooling, OC — oil cooling, WC — water cooling [67].

on the principle of magnetic levitation (maglev). The German system, *Transrapid*, uses vehicle-mounted steel core excitation electromagnets and stationary slotted armatures. Japanese MLX001 test train sets use onboard superconducting (SC) air-cored electromagnets and a stationary three-phase air-cored armature winding distributed along the guideway (Yamanashi Maglev Test Line).

A *linear stepping motor* has a concentrated armature winding wound on salient poles and PM excitation rail or variable reluctance platen (Fig. 1.4). The thrust is generated as an action of the armature magnetic flux and PM flux (active platen), or the armature magnetic flux and salient ferromagnetic poles (variable reluctance platen). Stepping motors have no position feedback.

The topology of a linear switched reluctance motor is similar to that of a stepping motor with variable reluctance platen. In addition, it is equipped with position sensors. The *turn-on* and *turn-off* instant of the input current is synchronized with the position of the moving part. The thrust is very sensitive to the turn-on and turn-off instant.

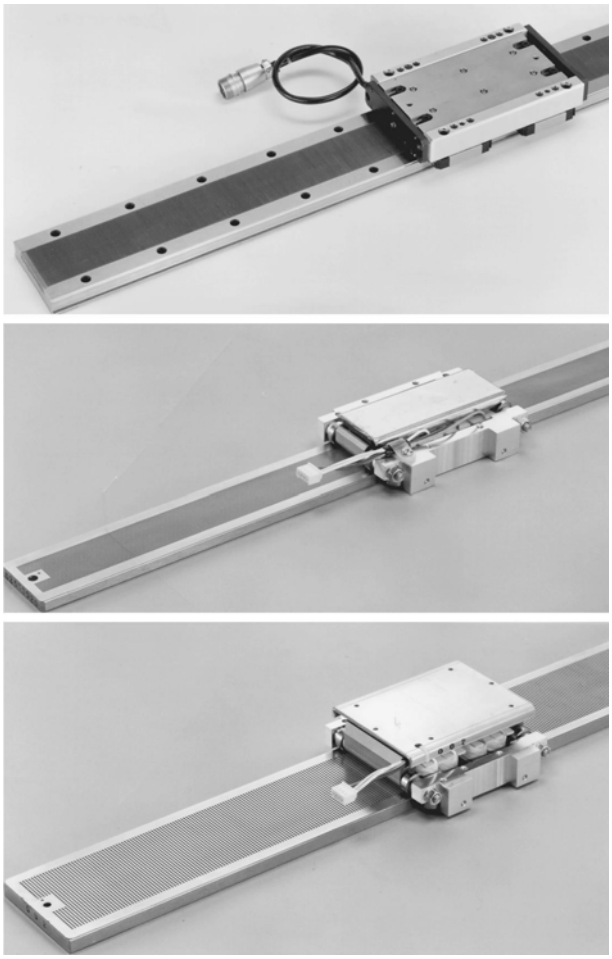

Fig. 1.4. PM linear stepping motors. Photo courtesy of Tokyo Aircraft Instrument, Co., Ltd., Japan.

In the case of a linear stepping or linear switched reluctance motor, the speed v of the moving part is

$$v = v_s = f_{sw}\tau \tag{1.4}$$

where f_{sw} is the fundamental switching frequency in one armature phase winding, and τ is the pole pitch of the reaction rail. For a rotary stepping or switched reluctance motor $f_{sw} = 2p_r n$, where $2p_r$ is the number of rotor poles and n is rotational speed in rev/s.

1.2 Linear Synchronous Motor Topologies

LSMs can be classified according to whether they are

- flat (planar) or tubular (cylindrical);
- single-sided or double-sided;
- slotted or slotless;
- iron cored or air cored;
- transverse flux or longitudinal flux.

The above topologies are possible for nearly all types of excitation systems. LSMs operating on the principle of the traveling magnetic field can have the following excitation systems:

- PMs in the reaction rail
- PMs in the armature (passive reaction rail)
- Electromagnetic excitation system (with winding)
- SC excitation system
- Passive reaction rail with saliency and neither PMs nor windings (variable reluctance motors)

LSMs with electronically switched d.c. armature windings are designed either as linear stepping motors or linear switched reluctance motors.

1.2.1 Permanent Magnet Motors with Active Reaction Rail

Fig. 1.5a shows a single-sided flat LSM with the armature winding located in slots and surface PMs. Fig. 1.5b shows a similar motor with buried-type PMs. In surface arrangement of PMs, the yoke (back iron) of the reaction rail is ferromagnetic, and PMs are magnetized in the normal direction (perpendicular to the active surface). Buried PMs are magnetized in the direction of the traveling magnetic field, and the yoke is nonferromagnetic, e.g., made of aluminum. Otherwise, the bottom leakage flux would be greater than the linkage flux, as shown in Fig. 1.6. The same effect occurs in buried type PM rotors of rotary machines in which the shaft must also be nonferromagnetic [70].

The so-called *Halbach array* of PMs also does not require any ferromagnetic yoke and excites stronger magnetic flux density and closer to the sinusoids than a conventional PM array [79]. The key concept of the Halbach array is that the magnetization vector should rotate as a function of distance along the array (Fig. 1.7).

It is recommended that be furnished a PM LSM with a *damper*. A rotary synchronous motor has a cage damper winding embedded in pole shoe slots. When the speed is different from the synchronous speed, electric currents are induced in damper circuits. The action of the armature magnetic field and damper currents allows for asynchronous starting, damps the oscillations,

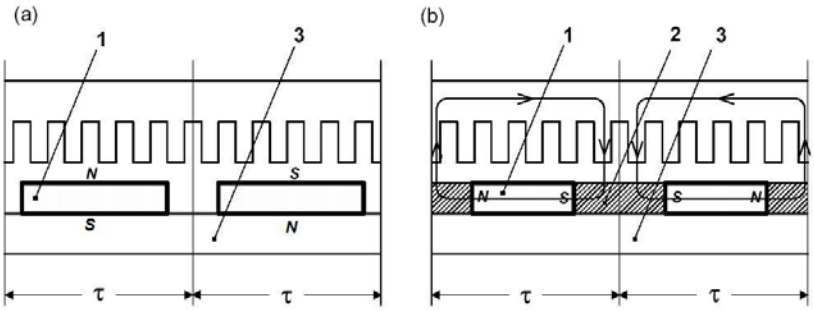

Fig. 1.5. Single sided flat PM LSMs with slotted armature core and (a) surface PMs, (b) buried PMs. 1 — PM, 2 — mild steel pole, 3 — yoke.

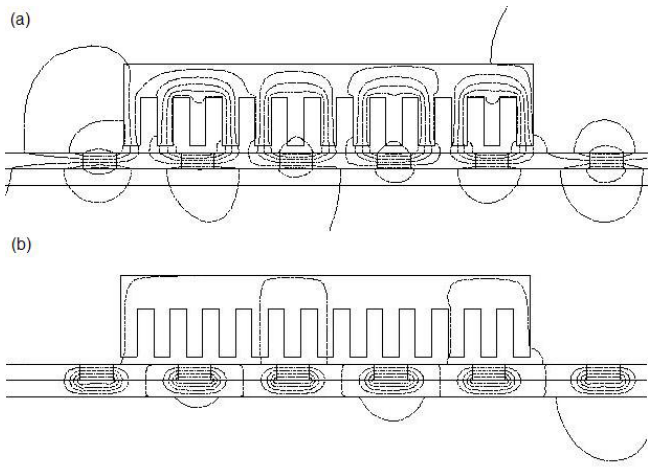

Fig. 1.6. Magnetic flux distribution in the longitudinal sections of buried-type PM LSMs: (a) nonferromagnetic yoke, (b) ferromagnetic yoke (back iron).

and helps to return to synchronous operation when the speed decreases or increases. Also, a damper circuit reduces the backward-traveling magnetic field. It would be rather difficult to furnish PMs with a cage winding so that the damper of PM LSMs has the form of an aluminum cover (Fig. 1.8a) or solid steel pole shoes (Fig. 1.8b). In addition, steel pole shoes or aluminum cover (shield) can protect brittle PMs against mechanical damage.

The *detent force*, i.e., attractive force between PMs and the armature ferromagnetic teeth, force ripple and some higher-space harmonics, can be reduced with the aid of skewed assembly of PMs. Skewed PMs can be arranged in one row (Fig. 1.9a), two rows (Fig. 1.9b), or even more rows.

Specification data of flat, single-sided PM LBMs manufactured by Anorad are shown in Table 1.1 [12], and motors manufactured by Kollmorgen are

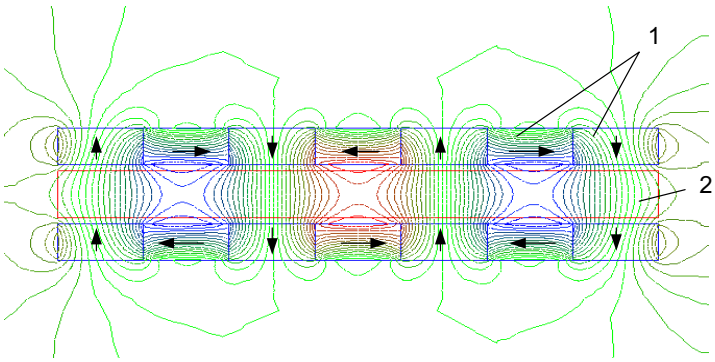

Fig. 1.7. Double-sided LSM with Halbach array of PMs. 1 — PMs, 2 — coreless armature winding.

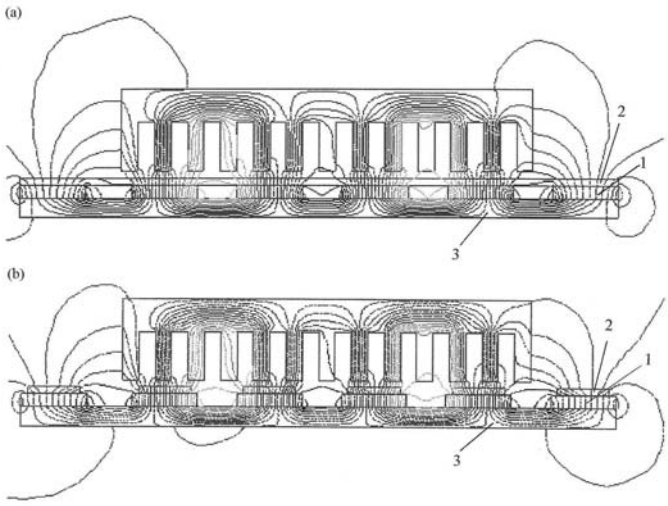

Fig. 1.8. Dampers of surface-type PM LSMs: (a) aluminum cover (shield), (b) solid steel pole shoes. 1 — PM, 2 — damper, 3 — yoke.

shown in Table 1.2 [112]. The temperature 25°C, 125°C, or 130°C for the thrust, current, resistance, and power loss is the temperature of the armature winding.

The EMF constant k_E in Tables 1.1 and 1.2 for sinusoidal operation is defined according to the equation expressing the EMF (induced voltage) excited by PMs without the armature reaction, i.e.,

$$E_f = c_E \Phi_f v_s = k_E v_s \tag{1.5}$$

Table 1.1. Flat three-phase, single-sided PM LBMs with natural cooling systems manufactured by Anorad, Hauppage, NY, USA

Parameter	LCD-T-1	LCD-T-2-P	LCD-T-3-P	LCD-T-4-P
Continuous thrust at 25°C, N	163	245	327	490
Continuous current at 25°C, A	4.2	6.3	8.5	12.7
Continuous thrust at 125°C, N	139	208	277	416
Continuous current at 125°C, A	3.6	5.4	7.2	10.8
Peak thrust (0.25 s), N	303	455	606	909
Peak current (0.25 s), A	9.2	13.8	18.4	27.6
Peak force (1.0 s), N	248	373	497	745
Peak current (1.0 s), A	7.3	11.0	14.7	22.0
Continuous power losses at 125°C, W	58	87	115	173
Armature constant, k_E, Vs/m	12.9			
Thrust constant (three phases), k_F N/A	38.6			
Resistance per phase at 25°C, Ω	3.2	2.2	1.6	1.1
Inductance, mH	14.3	9.5	7.1	4.8
PM pole pitch, mm	23.45			
Maximum winding temperature, °C	125			
Armature assembly mass, kg	1.8	2.4	3.6	4.8
PM assembly mass, kg/m	6.4			
Normal attractive force, N	1036	1555	2073	3109

Table 1.2. Flat three-phase, single-sided PM LBMs with natural cooling systems manufactured by Kollmorgen, Radford, VA, USA

Parameter	IC11-030	IC11-050	IC11-100	IC11-200
Continuous thrust at 130°C, N	150	275	600	1260
Continuous current at 130°C, A	4.0	4.4	4.8	5.0
Peak thrust, N	300	500	1000	2000
Peak current, A	7.9	7.9	7.9	7.9
Continuous power losses at 130°C, W	64	106	210	418
Armature constant, at 25^0C, k_E, Vs/m	30.9	51.4	102.8	205.7
Thrust constant (three phases) at 25°C, k_F, N/A	37.8	62.9	125.9	251.9
Resistance, line-to-line, at 25^0C, Ω	1.9	2.6	4.4	8.0
Inductance, line-to-line, mH	17.3	27.8	54.1	106.6
Electrical time constant, ms	8.9	10.5	12.3	13.4
Thermal resistance winding to external structure, ^{0}C/W	1.64	0.99	0.50	0.25
Maximum winding temperature, °C	130			
Armature assembly mass, kg	2.0	3.2	6.2	12.2
PM assembly mass, kg/m	5.5	7.6	12.8	26.9
Normal attractive force, N	1440	2430	4900	9850

Table 1.3. Slotted versus slotless LSMs

Quantity	Slotted LSM	Slotless LSM
Higher thrust density	x	
Higher efficiency in the lower speed range	x	
Higher efficiency in the higher speed range		x
Lower input current	x	
Less PM material	x	
Lower winding cost		x
Lower thrust pulsations		x
Lower acoustic noise		x

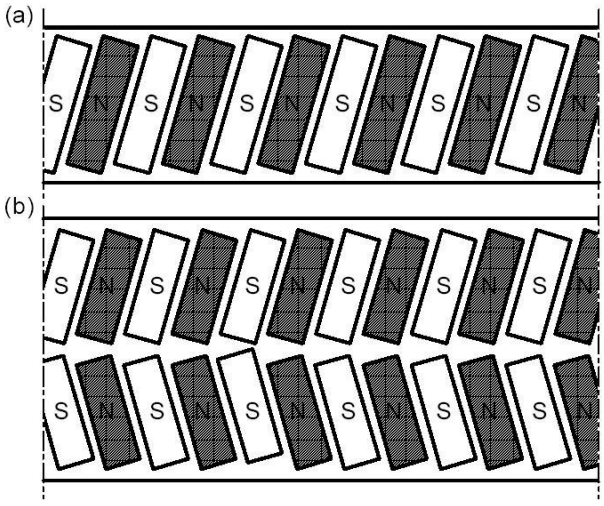

Fig. 1.9. Skewed PMs in flat LSMs: (a) one row, (b) two rows.

where Φ_f is the magnetic flux of the excitation system, and $k_E = c_E \Phi_f$. Thus, the armature constant k_E multiplied by the synchronous speed v_s gives the EMF E_f.

The thrust constant k_F in Tables 1.1 and 1.2 is defined according to the simplified equation for the electromagnetic thrust, i.e.,

$$F_{dx} = m_1 \frac{c_F}{2} \Phi_f I_a \cos\Psi = k_F I_a \cos\Psi \tag{1.6}$$

for a sinusoidally excited LSM with equal reluctances in the d- and q-axis and for the angle between the armature current I_a and the q-axis $\Psi = 0^0$ ($\cos\Psi = 1$). Thus, the thrust constant $k_F = 0.5 m_1 c_F \Phi_f$ times the armature current I_a gives the thrust. Derivations of eqns (1.5) and (1.6) are given in Chapter 6.

In the case of six degrees of freedom (DOF) as, for example, in planar PM actuators [39, 99] eqn (1.6) takes the matrix form, i.e.,

$$\begin{bmatrix} F_{dx} \\ F_{dy} \\ F_{dz} \\ T_{dx} \\ T_{dy} \\ T_{dz} \end{bmatrix} = \begin{bmatrix} k_{Fx}(x,y,z,\phi) \\ k_{Fy}(x,y,z,\phi) \\ k_{Fz}(x,y,z,\phi) \\ k_{Tx}(x,y,z,\phi) \\ k_{Ty}(x,y,z,\phi) \\ k_{Tz}(x,y,z,\phi) \end{bmatrix} \times I_a \tag{1.7}$$

where k_{Fx}, k_{Fy}, k_{Fz} are the thrust constants, and k_{Tx}, k_{Ty}, k_{Tz} are the torque constants in the x, y, and z directions, repectively.

Double-sided, flat PM LSMs consist of two external armature systems and one internal excitation system (Fig. 1.10a), or one internal armature system

Table 1.4. Flat double-sided PM LBMs with inner three-phase air-cored series-coil armature winding manufactured by Trilogy Systems Corporation, Webster, TX, USA

Parameter	310-2	310-4	310-6
Continuous thrust, N	111.2	209.1	314.9
Continuous power for sinusoidal operation, W	87	152	230
Peak thrust, N	356	712	1068
Peak power, W	900	1800	2700
Peak/continuous current, A	10.0/2.8	10.0/2.6	10.0/2.6
Thrust constant k_F for sinusoidal operation, N/A	40.0	80.0	120.0
Thrust constant k_F for trapezoidal operation with Hall sensors, N/A	35.1	72.5	109.5
Resistance per phase, Ω	8.6	17.2	25.8
Inductance ±0.5 mH	6.0	12.0	18.0
Heat dissipation constant for natural cooling, W/^{0}C	1.10	2.01	3.01
Heat dissipation constant for forced air cooling, W/°C	1.30	2.40	3.55
Heat dissipation constant for liquid cooling, W/°C	1.54	2.85	4.21
Number of poles	2	4	6
Coil length, mm	142.2	264.2	386.1
Coil mass, kg	0.55	1.03	1.53
Mass of PM excitation systems, kg/m	12.67 or 8.38		

and two external excitation systems (Fig. 1.10b). In the second case, a linear Gramme's armature winding can be used.

In *slotless motors* the primary winding is uniformly distributed on a smoooth armature core or does not have any armature core. Slotless PM LSMs are detent force free motors, provide lower torque ripple and, at high input frequency, can achieve higher efficiency than slotted LSMs. On the other hand, larger nonferromagnetic air gap requires more PM material, and the thrust density (thrust per mass or volume) is lower than that of slotted motors (Table 1.3). The input current is higher as synchronous reactances in the d- and q-axis can decrease to a low undesired value due to absence of teeth. Fig. 1.11a shows a single-sided flat slotless motor with armature core, and

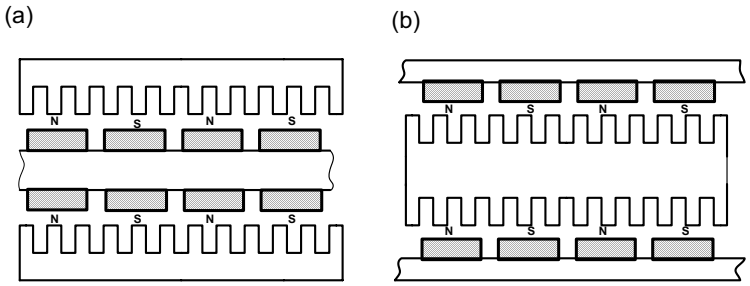

Fig. 1.10. Double-sided flat PM LSMs with: (a) two external armature systems, (b) one internal armature system.

Fig. 1.11b shows a double-sided slotless motor with inner air-cored armature winding (moving coil motor).

Table 1.4 contains performance specifications of double-sided PM LBMs with inner three-phase air-cored armature winding manufactured by Trilogy Systems Corporation, Webster, TX, USA [222]. Trilogy also manufactures motors with parallel wound coils as well as miniature motors and high-force motors (up to 9000 N continuous thrust).

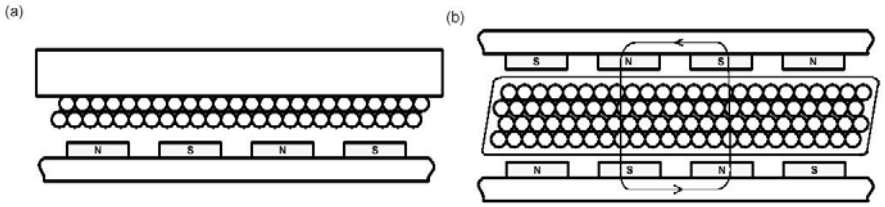

Fig. 1.11. Flat slotless PM LSMs: (a) single-sided with armature core, (b) double-sided with inner air-cored armature winding.

By rolling a flat LSM around the axis parallel to the direction of the traveling magnetic field, i.e., parallel to the direction of thrust, a tubular (cylindrical) LSM can be obtained (Fig. 1.12). A tubular PM LSM can also be designed as a double-sided motor or slotless motor.

Tubular single-sided LSMs LinMoT®[1] with movable internal PM excitation system (slider) and stationary external armature are manufactured by Sulzer Electronics AG, Zürich, Switzerland (Table 1.5). All active motor parts, bearings, position sensors, and electronics have been integrated into a rigid metal cylinder [125].

[1] LinMot®is a registered trademark of Sulzer Electronics AG, Zürich, Switzerland.

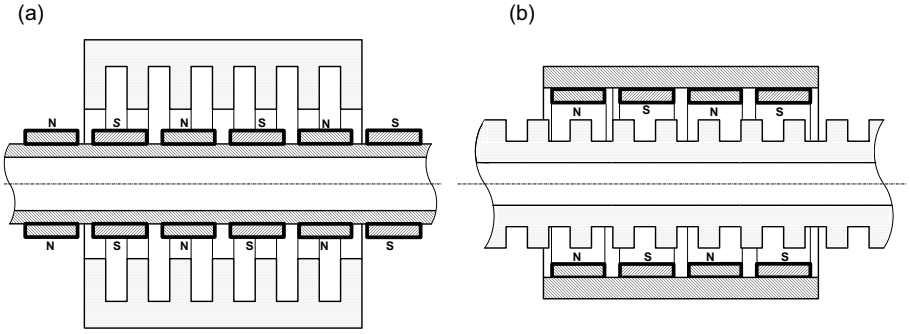

Fig. 1.12. Single-sided slotted tubular PM LSMs: (a) with external armature system, (b) with external excitation system.

Table 1.5. Data of tubular LSMs LinMot®manufactured by Sulzer Electronics AG, Zürich, Switzerland

Parameter	P01 23x80	P01 23X160	P01 37x120	P01 37x240
Number of phases	2			
Permanent magnets	NdFeB			
Maximum stroke, m	0.210	0.340	1.400	1.460
Maximum force, N	33	60	122	204
Maximum acceleration, m/s^2	280	350	247	268
Maximum speed, m/s	2.4	4.2	4.0	3.1
Stator (armature) length, m	0.177	0.257	0.227	0.347
Stator outer diameter, mm	23	23	37	37
Stator mass, kg	0.265	0.450	0.740	1.385
Slider diameter, mm	12	12	20	20
Maximum temperature of the armature winding, ^0C	90			

All the above-mentioned PM LSMs are motors with *longitudinal magnetic flux*, the lines of which lie in the plane parallel to the direction of the traveling magnetic field. LSMs can also be designed as *transverse magnetic flux* motors, in which the lines of magnetic flux are perpendicular to the direction of the traveling field. Fig. 1.13 shows a single-sided transverse flux LSM in which PMs are arranged in two rows. A pair of parallel PMs creates a two pole flux excitation system. A double-sided configuration of transverse flux motor is possible; however, it is complicated and expensive.

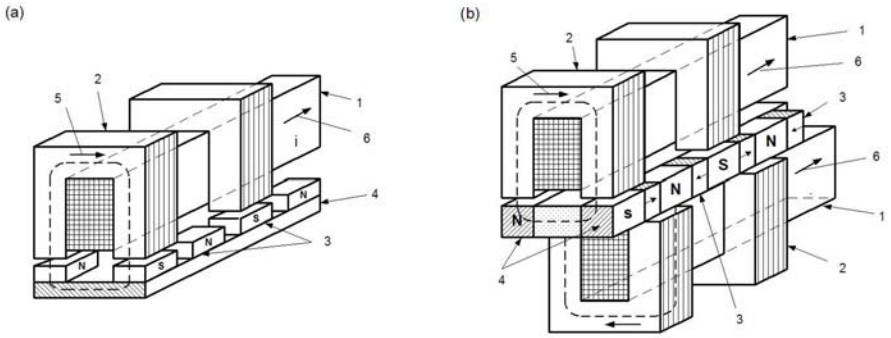

Fig. 1.13. Transverse flux PM LSM: (a) single-sided; (b) double-sided. 1 — armature winding, 2 — armature laminated core, 3 — PM, 4 — armature current, 5 — back ferromagnetic core, 6 — mild steel pole shoes, 7 — magnetic flux.

1.2.2 PM Motors with Passive Reaction Rail

The drawback of PM LSMs is the large amount of PM material that must be used to design the excitation system. Normally, expensive rare-earth PMs are requested. If a small PM LSM uses, say, 10 kg of NdFeB per 1 m of the reaction rail, and 1 kg of good-quality NdFeB costs US$ 130, the cost of the reaction rail without assembly amounts to US$ 1300 per 1 m. This price cannot be acceptable, e.g., in passenger transportation systems.

A cheaper solution is to apply the PM excitation system to the short armature that magnetizes the long reaction rail and creates magnetic poles in it. Such a linear motor is called the *homopolar* LSM.

The homopolar LSM as described in [59, 181] is a double-sided a.c. linear motor that consists of two polyphase armature systems connected mechanically and magnetically by a ferromagnetic U-type yoke (Fig. 1.14). Each armature consists of a typical slotted linear motor stack with polyphase armature winding and PMs located between the stack and U-type yoke. Since the armature and excitation systems are combined together, the armature stack is oversized as compared with a conventional steel-cored LSM. The PMs can also be replaced by electromagnets [181, 186]. The variable reluctance reaction rail is passive. The saliency is created by using ferromagnetic (solid or laminated) cubes separated by a nonferromagnetic material. The reaction rail poles are magnetized by the armature PMs through the air gap. The traveling magnetic field of the polyphase armature winding and salient poles of the reaction rail produce the thrust. Such a homopolar LSM has been proposed for the propulsion of maglev trains of *Swissmetro* [181].

Further simplification of the double-sided configuration can be made to obtain a single-sided PM LSM shown in Fig. 1.15.

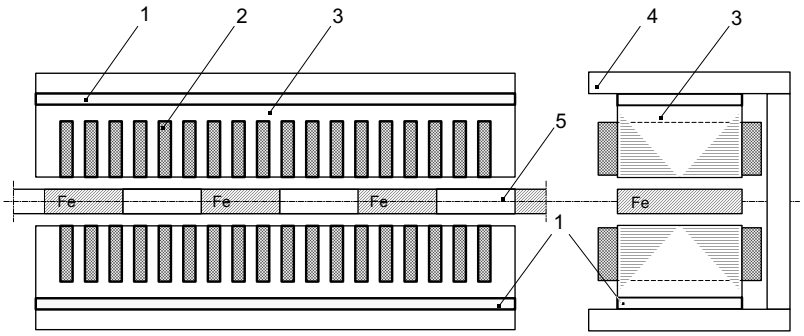

Fig. 1.14. Double-sided homopolar PM LSM with passive reaction rail. 1 — PM, 2 — armature winding, 3 — armature stack, 4 – yoke, 5 — reaction rail.

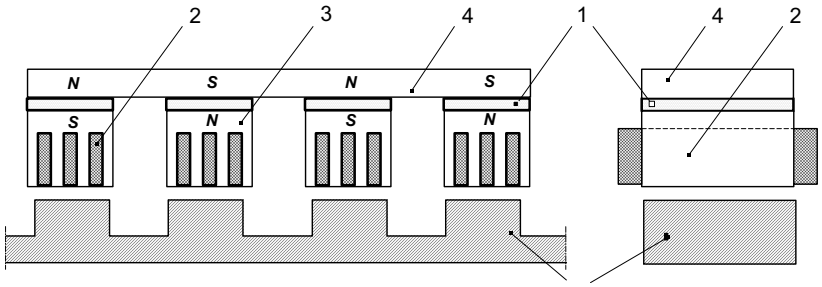

Fig. 1.15. Single-sided PM LSM with a passive reaction rail. 1 — PM, 2 — armature winding, 3 — armature stack, 4 — yoke, 5 — ferromagnetic reaction rail.

1.2.3 Motors with Electromagnetic Excitation

The electromagnetic excitation system of an LSM is similar to the salient pole rotor of a rotary synchronous motor. Fig. 1.16 shows a flat single-sided LSM with salient ferromagnetic poles and *d.c. field excitation winding*. The poles and pole shoes can be made of solid steel, laminated steel, or sintered powder. If the electromagnetic excitation system is integrated with the moving part, the d.c. current can be delivered with the aid of brushes and contact bars, inductive power transfer (IPT) systems [201], linear transformers, or linear brushless exciters.

1.2.4 Motors with Superconducting Excitation System

In large-power LSMs, the electromagnets with ferromagnetic core that produce the excitation flux can be replaced by coreless *superconducting* (SC) electromagnets. Since the magnetic flux density produced by the SC electromagnet is greater than the saturation magnetic flux density of the best

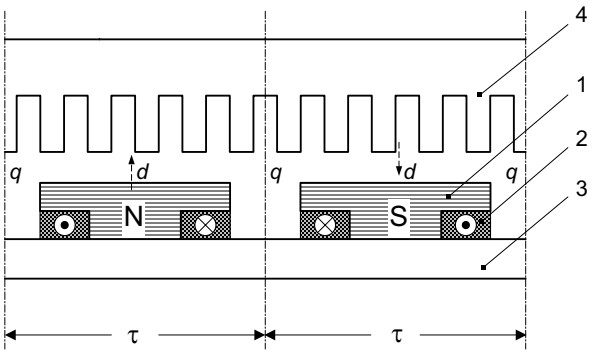

Fig. 1.16. Electromagnetic excitation system of a flat single-sided iron-cored LSM. 1 — salient pole, 2 — d.c. excitation winding, 3 — ferromagnetic rail (yoke), 4 — armature system.

laminated alloys ($B_{sat} \approx 2.4$ T for cobalt alloy), there is no need to use the armature ferromagnetic core. An LSM with SC field excitation system is a totally air-cored machine (Fig. 1.17).

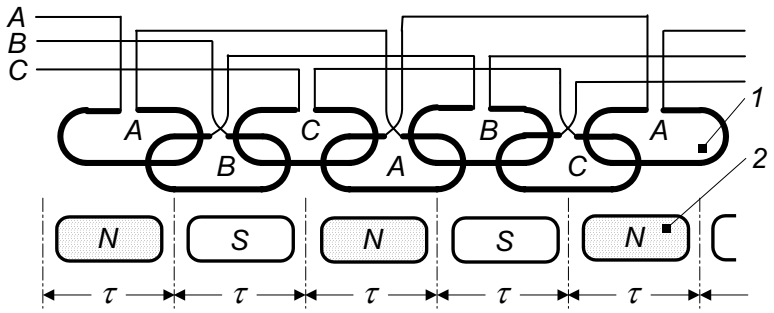

Fig. 1.17. Three-phase air-cored LSM with SC excitation system. 1 — armature coils, 2 — SC excitation coils.

1.2.5 Variable Reluctance Motors

The simplest construction of a *variable reluctance LSM* or *linear reluctance motor* (LRM) is that shown in Fig. 1.16 with d.c. excitation winding being removed. However, the thrust of such a motor would be low as the ratio of d-axis permeance to q-axis permeance is low. Better performance can be obtained when using *flux barriers* [183] or steel laminations [127]. To make

flux barriers, any nonferromagnetic materials can be used. To obtain high permeance (low reluctance) in the d-axis and low permeance in the q-axis, steel laminations should be oriented in such a way as to create high permeance for the d-axis magnetic flux.

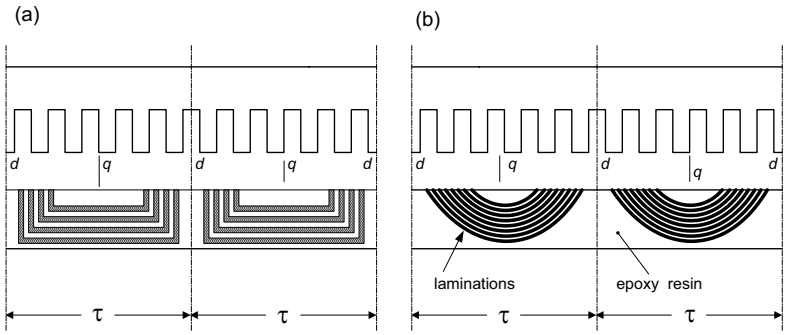

Fig. 1.18. Variable reluctance LSMs with (a) flux barriers, (b) steel laminations.

Fig. 1.18a shows a variable reluctance platen with flux barriers, and Fig. 1.18b shows how to arrange steel laminations to obtain different reluctances in the d- and q-axis. The platen can be composed of segments the length of which is equal to the pole pitch τ. Each segment consists of semicircular *lamellas* cut out from electrotechnical sheet. A filling, e.g., epoxy resin, is used to make the segment rigid and robust. By putting the segments together, a platen of any desired length can be obtained [81].

1.2.6 Stepping Motors

So far, only stepping linear motors of hybrid construction (PM, winding and variable reluctance air gap) have found practical applications.

The *hybrid linear stepping motor* (HLSM), as shown in Fig. 1.19, consists of two parts: the *forcer* (also called the *slider*) and the variable reluctance platen [40]. Both of them are evenly toothed and made of high-permeability steel. This is an early design of the HLSM, the so-called Sawyer linear motor [88]. The forcer is the moving part with two rare-earth magnets and two concentrated parameter windings. The tooth pitch of the forcer matches the tooth pitch on the platen. However, the tooth pitches on the forcer poles are spaced 1/4 or 1/2 pitch from one pole to the next. This arrangement allows for the PM flux to be controlled at any level between minimum and maximum by the winding so that the forcer and the platen line up at a maximum permeance position. The HLSM is fed with two-phase currents (90° out of phase), similarly as a rotary stepping motor. The forcer moves 1/4 tooth pitch per each full step.

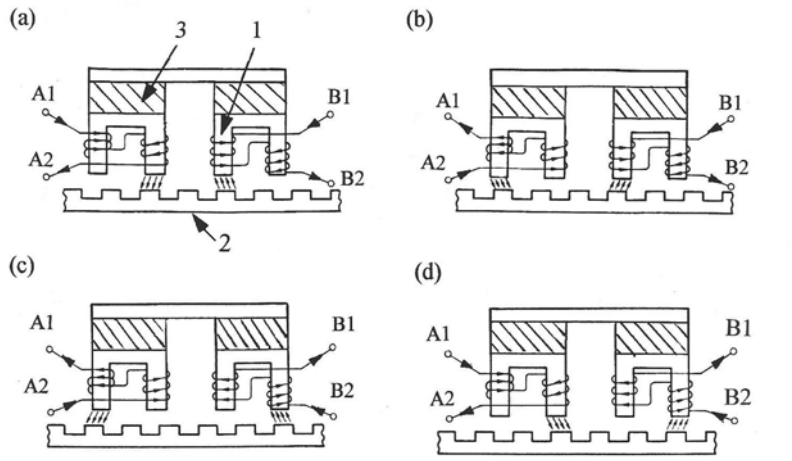

Fig. 1.19. Principle of operation of an HLSM: (a) initial position; (b) 1/4 tooth pitch displacement of the forcer; (c) 2/4 tooth pitch displacement; (d) 3/4 tooth pitch displacement. 1 — forcer, 2 — platen, 3 — PM.

There is a very small air gap between the two parts that is maintained by strong air flow produced by an air compressor [102]. The average air pressure is about 300 to 400 kpa and depends on how many phases are excited.

Table 1.6 shows specification data of HLSMs manufactured by Tokyo Aircraft Instrument Co., Ltd., Tokyo, Japan [122]. The *holding force* is the amount of external force required to break the forcer away from its rest position at rated current applied to the motor. The *step–to–step accuracy* is a measure of the maximum deviation from the true position in the length of each step. This value is different for full-step and microstepping drives. The *maximum start—stop speed* is the maximum speed that can be used when starting or stopping the motor without ramping that does not cause the motor to fall out of synchronism or lose steps. The *maximum speed* is the maximum linear speed that can be achieved without the motor stalling or falling out of synchronism. The *maximum load mass* is the maximum allowable mass applied to the forcer against the scale that does not result in mechanical damage. The *full-step resolution* is the position increment obtained when the currents are switched from one winding to the next winding. This is the typical resolution obtained with full-step drives and it is strictly a function of the motor construction. The *microstepping resolution* is the position increment obtained when the full-step resolution is divided electronically by proportioning the currents in the two windings (Chapter 6). This resolution is typically 10 to 250 times smaller than the full-step resolution [122].

HLSMs are regarded as an excellent solution to positioning systems that require a high accuracy and rapid acceleration. With a microprocessor controlled *microstepping mode* (Chapter 6), a smooth operation with standard

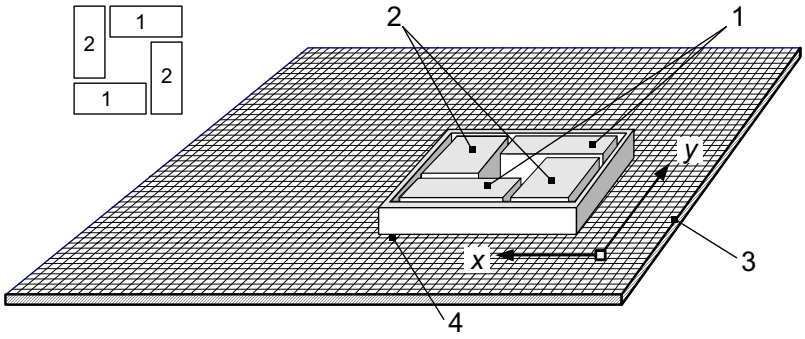

Fig. 1.20. HLSM with a four-unit forcer to obtain the x-y motion: 1 — forcers for the x-direction, 2 — forcers for the y–direction, 3 — platen, 4 — air pressure.

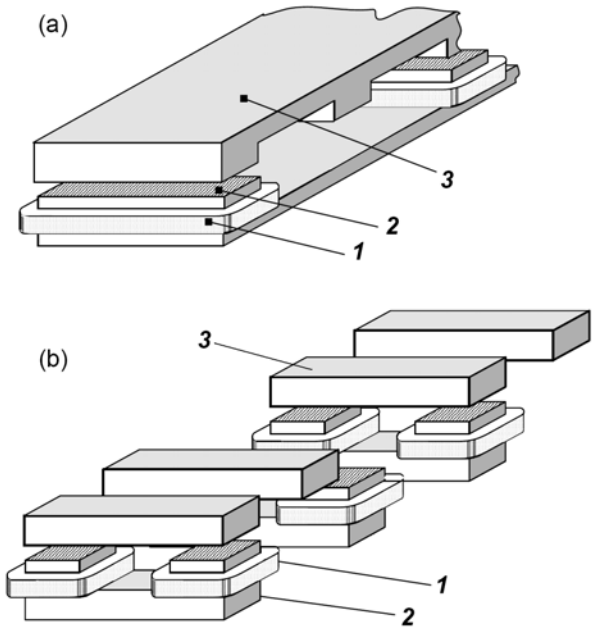

Fig. 1.21. Linear switched reluctance motor configurations: (a) longitudinal flux design, (b) transverse flux design. 1 — armature winding, 2 — armature stack, 3 — platen.

Table 1.6. Data of HLSMs manufactured by Tokyo Aircraft Instrument Co., Ltd., Tokyo, Japan.

Parameter	LP02-20A	LP04-20A	LP04-30A	LP60-20A
Driver	Bi-Polar Chopper			
Voltage, V	24 d.c.			
Resolution, mm	0.2	0.4	0.4	0.423
Holding Force, N	20	20	29.5	20
Step-to-step accuracy, mm	±0.03			
Comulative accuracy, mm	±0.2			
Maximum start-stop speed, mm/s	60	120	120	127
Maximum speed, mm/s	400	600	500	600
Maximum load mass, kg	3.0	3.0	5.0	3.0
Effective stroke, mm	330	300	360	310
Mass, kg	1.4	1.2	2.8	1.4

resolution of a few hundred steps/mm can be obtained. The advantages such as high efficiency, high throughput, mechanical simplicity, high reliability, precise open-loop operation, low inertia of the system, etc, have made these kind of motors more and more attractive in such applications as factory automation, high speed positioning, computer peripherals, facsimile machines, numerically controlled machine tools, automated medical equipment, automated laboratory equipment and welding robots. This motor is especially suitable for machine tools, printers, plotters and computer controlled material handling in which a high positioning accuracy and repeatability are the key problems.

When two or four forcers mounted at 90° and a special grooved platen ("waffle plate") are used, the *x-y* motion (two DOFs) in a single plane is obtained (Fig. 1.20). Specification data of the *x-y* HLSMs manufactured by Normag Northern Magnetics, Inc., Santa Clarita, CA, USA are given in Table 1.7 [161].

1.2.7 Switched Reluctance Motors

A *linear switched reluctance motor* has a doubly salient magnetic circuit with a polyphase winding on the armature. Longitudinal and transverse flux designs are shown in Fig. 1.21. A linear switched reluctance motor allows precise speed and position-controlled linear motion at low speeds and is not subject to design constraints (minimum speed limited by minimum feasible pole pitch) of linear a.c. motors [4].

Table 1.7. Data of $x-y$ HLSMs manufactured by Normag Northern Magnetics, Inc., Santa Clarita, CA, USA

Parameter	4XY0602-2-0	4XY2002-2-0	4XY2004-2-0	4XY2504-2-0
Number of forcer units per axis	1	1	2	2
Number of phases	2	2	2(4)	2(4)
Static thrust, N	13.3	40.0	98.0	133.0
Thrust at 1m/s, N	11.1	31.1	71.2	98.0
Normal attractive force, N	160.0	400.0	1440.0	1800.0
Resistance per phase, Ω	2.9	3.3	1.6	1.9
Inductance per phase, mH	1.5	4.0	2.0	2.3
Input phase current, A	2.0	2.0	4.0	4.0
Air gap, mm	0.02			
Maximum temperature, °C	110			
Mass, kg	3.2	0.72	2.0	1.5
Repeatability, mm	0.00254			
Resolution, mm	0.00254			
Bearing type	air			

1.3 Calculation of Forces

Neglecting the core loss and nonlinearity, the *energy stored in the magnetic field* is

$$W = \frac{1}{2}\Phi\mathcal{F} = \frac{1}{2}\Phi Ni \qquad \text{J} \tag{1.8}$$

where the magnetomotive force (MMF) $\mathcal{F} = Ni$. Introducing the reluctance $\Re = \mathcal{F}/\Phi$, the field energy is

$$W = \frac{1}{2}\Re\Phi^2 = \frac{1}{2}\frac{\mathcal{F}^2}{\Re} \qquad \text{J} \tag{1.9}$$

The self-inductance

$$L = \frac{N\Phi}{i} \tag{1.10}$$

is constant for $\Re = const$. Hence,

$$W = \frac{1}{2}Li^2 \tag{1.11}$$

In a magnetic circuit with air gap $g > 0$, most of the MMF is expended on the air gap and most of the energy is stored in the air gap with its volume Ag where A is the cross section area of the air gap. Working in B and H units, the field energy per volume is

$$w = \frac{W}{Ag} = \frac{1}{2}B_g H = \frac{1}{2}\frac{B_g^2}{\mu_0} \qquad \text{J/m}^3 \tag{1.12}$$

where B_g is the magnetic flux density in the air gap.

The magnetic quantities corresponding to electric quantities are listed in Table 1.8.

Table 1.8. Electric and corresponding magnetic quantities

Electric circuit	Unit	Magnetic circuit	Unit
Electric voltage, $V = \int_l Edl$	V	Magnetic voltage, $V_\mu = \int_l Hdl$	A
EMF, E	V	MMF, $\mathcal{F}$	A
Current, I	A	Magnetic flux, Φ	Wb
Current density, J	A/m^2	Magnetic flux density, B	Wb/m^2=T
Resistance, R	Ω	Reluctance, $\Re$	1/H
Conductance, G	S	Permeance, G	H
Electric conductivity, ρ	S/m	Magnetic permeability, μ	H/m

The *force F_i associated with any linear motion* defined by a variable ξ_i of a device employing a magnetic field is given by

$$F_i = \frac{\partial W}{\partial \xi_i} \tag{1.13}$$

where W is the field energy in Joules according to eqn (1.8), F_i denotes the F_x, F_y, or F_z force component and ξ_i denotes the x, y, or z coordinate.

For a singly excited device

$$F_i = \frac{1}{2}\Phi^2\frac{d\Re}{d\xi_i} = \frac{1}{2}i^2\frac{dL}{d\xi_i} \tag{1.14}$$

where the magnetic flux $\Phi = const$, and electric current $i = const$.

Eqn (1.14) can be used to find the attractive force between two poles separated by an air gap $z = g$. Let us consider a linear electromagnetic actuator, electromagnet, or relay mechanism. The following assumptions are usually made: (a) leakage flux paths are neglected, (b) nonlinearities are neglected, and (c) all the field energy is stored in the air gap ($\mu_0\mu_r >> \mu_0$) where the magnetic permeability of free space $\mu_0 = 0.4\pi \times 10^{-6}$ H/m, and μ_r is the relative permeability. The volume of the air gap is Az, and the stored field

energy is $W = 0.5(B_g^2/\mu_0)Az$. For a U-shaped electromagnet (two air gaps) the stored field energy is $W = 0.5(B_g^2/\mu_0)2Az = (B_g^2/\mu_0)Az$. With the displacement dz of one pole, the new air gap is $z + dz$, new stored energy is $W + dW = (B_g^2/\mu_0)A(z + dz)$, change in stored energy is $(B_g^2/\mu_0)Adz$, work done $F_z dz$ and the force

$$F_z = \frac{dW}{dz} = \frac{B_g^2}{\mu_0}A = \frac{1}{4}\frac{\mu_0(Ni)^2}{g^2}A \tag{1.15}$$

where $B_g = \mu_0 H = \mu_0[Ni/(2z)]$, $z = g$, i is the instantaneous electric current, and A is the cross section of the air gap (surface of a single pole shoe). Eqn (1.15) is used to find the normal (attractive) force between the armature core and reaction rail of linear motors. For a doubly excited device,

$$F_i = \frac{1}{2}i_1^2\frac{dL_{11}}{d\xi_i} + \frac{1}{2}i_2^2\frac{dL_{22}}{d\xi_i} + i_1 i_2\frac{dL_{12}}{d\xi_i} \tag{1.16}$$

where L_{11} is the self-inductance of the winding with current i_1, L_{22} is the self-inductance of the winding with current i_2, and L_{12} is the mutual inductance between coils 1 and 2. In simplified calculations, the first two terms are commonly zero.

1.4 Linear Motion

1.4.1 Speed-Time Curve

The *speed-time curve* is a graph that shows the variation of the linear speed versus time (Fig. 1.22a). In most cases, both for acceleration and deceleration periods, the speed is a linear function of time. Thus, the speed-time curve of a moving object is most often approximated by a trapezoidal function (Fig. 1.22a). The acceleration time is

$$t_1 = \frac{v_{const}}{a} \tag{1.17}$$

where v_{const} is the constant (steady state) speed. Similarly, the retardation time is

$$t_3 = \frac{v_{const}}{d} \tag{1.18}$$

where d is the deceleration. The time t_2 for a constant-speed running depends both on acceleration and deceleration, i.e.,

$$t_2 = t - t_1 - t_3 = t - v_{const}\left(\frac{1}{a} + \frac{1}{d}\right) \tag{1.19}$$

where the total time of run $t = t_1 + t_2 + t_3$. The total distance of run can be found on the basis of Fig. 1.22a, i.e.,

$$s = \frac{1}{2}v_{const}t_1 + v_{const}t_2 + \frac{1}{2}v_{const}t_3 = v_{const}t - \frac{v_{const}^2}{2}\left(\frac{1}{a} + \frac{1}{d}\right) \tag{1.20}$$

or

$$kv_{const}^2 - tv_{const} + s = 0 \tag{1.21}$$

where

$$k = \frac{1}{2}\left(\frac{1}{a} + \frac{1}{d}\right) \tag{1.22}$$

The above quadratic eqn (1.21) allows one to find the constant speed as a function of the total time of run, acceleration, deceleration, and total distance of run, i.e.,

$$v_{const} = \frac{t}{2k} - \sqrt{\left(\frac{t}{2k}\right)^2 - \frac{s}{k}} \tag{1.23}$$

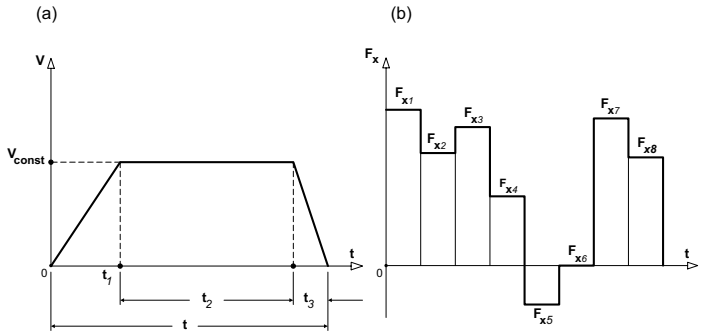

Fig. 1.22. Typical speed and thrust profiles: (a) speed-time curve, (b) thrust-time curve.

Table 1.9 compares basic formulae describing linear and rotational motions. There are two components of the linear acceleration: tangential $a = \alpha r$ and centripetal $a_r = \Omega^2 r$, where r is the radius.

1.4.2 Thrust-Time Curve

The *thrust-time curve* is a graph that shows the variation of the thrust versus time (Fig. 1.22b). The *rms* thrust (force in the x-direction) is based on the given duty cycle, i.e.,

Table 1.9. Basic formulae for linear and rotational motions

Linear motion			Rotational motion		
Quantity	Formula	Unit	Quantity	Formula	Unit
Linear displacement	$s = \theta r$	m	Angular displacement	θ	rad
Linear velocity	$v = ds/dt$ $v = \Omega r$	m/s	Angular velocity	$\Omega = d\theta/dt$	rad/s
Linear acceleration	$a = dv/dt$ $a_t = \alpha r$ $a_r = \Omega^2 r$	m/s^2	Angular acceleration	$\alpha = d\Omega/dt$	rad/s^2
Mass	m	kg	Moment of inertia	J	kgm^2
Force	$F = mdv/dt$ $= ma$	N	Torque	$T = Jd\Omega/dt$ $= J\alpha$	Nm
Momentum	$p = mv$	Ns	Angular momentum	$l = J\Omega$	kgm^{2}rad/s
Friction force	Dds/dt $= Dv$	N	Friction torque	$Dd\theta/dt$ $= D\Omega$	Nm
Spring force	Ks	N	Spring torque	$K\theta$	Nm
Work	$dW = Fds$	Nm	Work	$dW = Td\theta$	Nm
Kinetic energy	$E_k = 0.5mv^2$	J or Nm	Kinetic energy	$E_k = 0.5J\Omega^2$	J
Power	$P = dW/dt$ $= Fv$	W	Power	P = dW/dt $= T\Omega$	W

$$F_{xrms}^2 \sum t_i = \sum F_{xi}^2 t_i$$

$$F_{xrms} = \sqrt{\frac{F_{x1}^2 t_1 + F_{x2}^2 t_2 + F_{x3}^2 t_3 + ... + F_{xn}^2 t_n}{t_1 + t_2 + t_3 + ... + t_n}} \tag{1.24}$$

Similarly, in electric circuits, the rms or effective current is

$$I_{rms} = \sqrt{\frac{1}{T}\int_0^T i^2 dt}$$

since the average power delivered to the resistor R is

$$P = \frac{1}{T}\int_0^T i^2 R dt = R\frac{1}{T}\int_0^T i^2 dt = RI_{rms}^2$$

1.4.3 Dynamics

Fig. 1.23 shows the mass m sliding at velocity v with a viscous friction constant D_v on a surface. The applied instantaneous force is f_x, and the spring constant is k_s. According to d'Alembert's principle [2]

$$m\frac{dv}{dt} + D_v v + k_s \int v dt = F_x t \tag{1.25}$$

The above equation can also be written as

$$m\ddot{x} + D_v \dot{x} + k_s x = F_x t \tag{1.26}$$

where $\ddot{x} = d^2x/dt^2$ is the linear acceleration, $\dot{x} = dx/dt$ is the linear velocity, and x is the linear displacement. Eqns (1.25) and (1.26) are called *2nd order mass—spring—damper equations*. The inverse of stiffness (N/m) is the compliance (m/N) of an elastic element. The form of eqn (1.25) is similar to Kirchhoff's voltage equation for the RLC series circuit, i.e.,

$$L\frac{di}{dt} + Ri + \frac{1}{C}\int i dt = e \tag{1.27}$$

where e is the instantaneous induced voltage (EMF), and i is the instantaneous current. Since

$$v = \frac{dx}{dt} \qquad \text{and} \qquad i = \frac{dq}{dt}$$

where q is the electrical charge, eqns (1.25) and (1.27) can be rewritten in the forms

$$m\frac{d^2x}{dt^2} + D_v\frac{dx}{dt} + k_s x = F_x \tag{1.28}$$

$$L\frac{d^2q}{dt^2} + R\frac{dq}{dt} + \frac{1}{C}q = e \tag{1.29}$$

Analogous systems are described by the same integro-differential equation or set of equations, e.g., mechanical and electrical systems.

In the mechanical system, energy stored in the mass is given by the kinetic energy $0.5mv^2$. Energy storage occurs in a spring from the displacement $x = \int v dt$, due to a force. This force is expressed in terms of the stiffness of spring k_s, as $f_x = k_s x = k_s \int v dt$.

Assuming a linear force-displacement relation, the work done is

$$W = \frac{1}{2} f_x x = \frac{1}{2}\frac{1}{k_s} f_x^2 \qquad \text{J} \tag{1.30}$$

[2] d'Alambert's principle: The sum of forces acting on a body and forces of inertia is equal to zero.

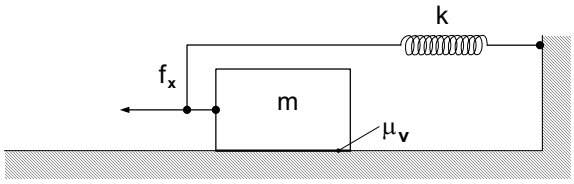

Fig. 1.23. A simple linear mechanical system.

A viscous friction element, such as a *dashpot*, is an energy-dissipating element. In the *mass–inductance analogy*, the inductance has stored electromagnetic energy $0.5Li^2$. Application of a voltage to a capacitance causes a proportional storage of charge, $q = \int idt$, and the voltage component is $(1/C)\int idt$.

Similarly, in the *mass–capacitance analogy*, the energy stored in a capacitance is $0.5Ce^2$. The energy storage of a spring, $0.5(1/k_s)f_x^2$, is analogous to that in the inductance, $0.5Li^2$, whence the inductance becomes the analogue of spring *compliance* ($K = 1/k_s$).

1.4.4 Hamilton's Principle

The action integral

$$I = \int_{t_1}^{t_2} \mathcal{L} dt \tag{1.31}$$

has a stationary value for the correct path of motion, where $\mathcal{L}$ is the *Lagrangian*, so

$$\delta I = \delta \int_{t_1}^{t_2} \mathcal{L} dt = 0 \tag{1.32}$$

Mathematically, eqn (1.32) means that the variation of the action integral is equal to zero. Eqn (1.32) expresses the *principle of least action*, also called Hamilton's principle.[3] The Lagrangian of a mechanical system is defined as

$$\mathcal{L} = E_k - E_p \tag{1.33}$$

where E_k is the total kinetic energy, and E_p is the total potential energy.

Hamilton's principle can be extended to electromechanical systems. The Lagrangian of an electromechanical system is defined as

[3] The principle of least action was proposed by the French mathematician and astronomer Pierre-Louis Moreau de Maupertuis but rigorously stated only much later, especially by the Irish mathematician and scientist William Rowan Hamilton in 1835.

$$\mathcal{L} = \int_V (H^2 - E^2) dV \tag{1.34}$$

where H is the magnetic field intensity, E is the electric field intensity, and v is the volume. The principle of least action for electromechanical systems,

$$\delta I = \delta \int_{t_1}^{t_2} \left[\int_V (H^2 - E^2) dV \right] dt = 0 \tag{1.35}$$

was formulated by J. Larmor in 1890 and is called Larmor's principle.

1.4.5 Euler–Lagrange Equation

The Euler–Lagrange differential equation is the fundamental equation of variations in calculus. It states that if J is defined by an integral of the form

$$J = \int f[\xi(t), \dot{\xi(t)}, t] dt \tag{1.36}$$

where ξ is the generalized coordinate and

$$\dot{\xi} = \frac{d\xi}{dt}$$

then J has a stationary value if the differential equation

$$\frac{\partial f}{\partial \xi} - \frac{d}{dt}\left(\frac{\partial f}{\partial \dot{\xi}}\right) = 0 \tag{1.37}$$

is satisfied. The Euler–Lagrange eqn (1.37) is expressed in time-derivative notation.

Hamilton's principle, also called the *principle of least action*, derived from d'Alambert's principle and the principle of *virtual work*, means that, for a real motion, the variation of action is equal to zero, i.e.,

$$\delta J = \delta \int \mathcal{L}(\xi, \dot{\xi}, t) = 0 \tag{1.38}$$

where $\mathcal{L} = E_k - E_p$ is called Lagrangian and is defined as a difference between kinetic and potential energy (1.33), or kinetic coenergy and potential energy.

Proof of Euler–Lagrange differential equation is given below.

$$\delta J = \delta \int_{t1}^{t2} \mathcal{L}(\xi, \dot{\xi}, t) dt = \int_{t1}^{t2} \left(\frac{\partial \mathcal{L}}{\partial \xi} \delta\xi + \frac{\partial \mathcal{L}}{\partial \dot{\xi}} \delta\dot{\xi} \right) dt$$

$$= \int_{t1}^{t2} \left[\frac{\partial \mathcal{L}}{\partial \xi} \delta\xi + \frac{\partial \mathcal{L}}{\partial \dot{\xi}} \frac{d}{dt}(\delta\xi) \right] dt \tag{1.39}$$

since $\delta\dot{\xi} = d(\delta\xi)/dt$. Now integrate the second term by parts using

$$u = \frac{\partial \mathcal{L}}{\partial \dot{\xi}} \qquad dv = d(\delta\xi)$$

$$du = \frac{d}{dt}\left(\frac{\partial \mathcal{L}}{\partial \dot{\xi}}\right) dt \qquad v = \delta\xi$$

because

$$d(uv) = udv + vdu \qquad \int_a^b udv = uv\Big|_a^b - \int_a^b vdu$$

Therefore,

$$\delta J = \frac{\partial \mathcal{L}}{\partial \dot{\xi}}\delta\xi\Big|_{t_1}^{t_2} + \int_{t_1}^{t_2}\left(\frac{\partial \mathcal{L}}{\partial \xi}\delta\xi - \frac{d}{dt}\frac{\partial \mathcal{L}}{\partial \dot{\xi}}\delta\xi\right) dt \tag{1.40}$$

Only the path, not the endpoints, varies. So, $\delta\xi(t_1) = \delta\xi(t_2) = 0$, and (1.40) becomes

$$\delta J = \int_{t_1}^{t_2}\left(\frac{\partial \mathcal{L}}{\partial \xi} - \frac{d}{dt}\frac{\partial \mathcal{L}}{\partial \dot{\xi}}\right)\delta\xi dt \tag{1.41}$$

Stationary values such that $\delta J = 0$ must be found. These must vanish for any small change δq, which gives from (1.41)

$$\frac{\partial \mathcal{L}}{\partial \xi} - \frac{d}{dt}\frac{\partial \mathcal{L}}{\partial \dot{\xi}} = 0$$

or

$$\frac{d}{dt}\frac{\partial \mathcal{L}}{\partial \dot{\xi}} - \frac{\partial \mathcal{L}}{\partial \xi} = 0 \tag{1.42}$$

Eqn (1.42) is the Euler–Lagrange differential equation. Problems in the calculus of variations often can be solved by solution of the appropriate Euler–Lagrange equation.

The Euler–Lagrange equation for nonconservative systems, in which external forces and dissipative elements exist, takes the form

$$\frac{d}{dt}\left[\frac{\partial \mathcal{L}(\dot{\xi}, \xi, t)}{\partial \dot{\xi}_k}\right] - \frac{\partial \mathcal{L}(\dot{\xi}, \xi, t)}{\partial \xi_k} + \frac{\partial Ra(\dot{\xi}, \xi, t)}{\partial \dot{\xi}_k} = Q_k \tag{1.43}$$

in which the first term on the left-hand side represents forces of inertia of the system, the second term represents spring forces, the third term represents forces of dissipation, and Q_k on the right-hand side represents external forces. The Rayleigh dissipation function is defined as

$$Ra = \frac{1}{2}R\dot{\xi}^2 + \frac{1}{2}D_v\dot{\xi}^2 \tag{1.44}$$

where R is the electric resistance and D_v is the mechanical dumping, e.g., viscous friction.

1.4.6 Traction

Let us consider a mechanism driven by a linear motor (Fig. 1.24a). The mechanism consists of a moving part, i.e., a linear–motor–driven car with the total mass m on a slope, a pulley, a cable, and a counterweight with its mass m_c. The efficiency of the system is η. The inertia of the pulley, and mass of the cable are neglected.

For the steady-state linear motion,

$$\eta(F_x + m_c g) = mg\sin\alpha + \mu mg\cos\alpha \tag{1.45}$$

where $mg\sin\alpha$ is the force due to the gradient resistance, $\mu mg\cos\alpha$ is the force due to the friction resistance, and $g = 9.81$ m/s^2 is the gravitational acceleration. The coefficient of friction μ is approximately 0.2 for steel on dry steel, 0.06 for steel on oiled steel (viscous friction), 0.005 for linear bearings with rollers, and 0.002 to 0.004 for linear bearings with balls. Thus, the steady-state thrust (force produced by the linear motor) is

$$F_x = \frac{1}{\eta}(m\sin\alpha + \mu m\cos\alpha - m_c)g \tag{1.46}$$

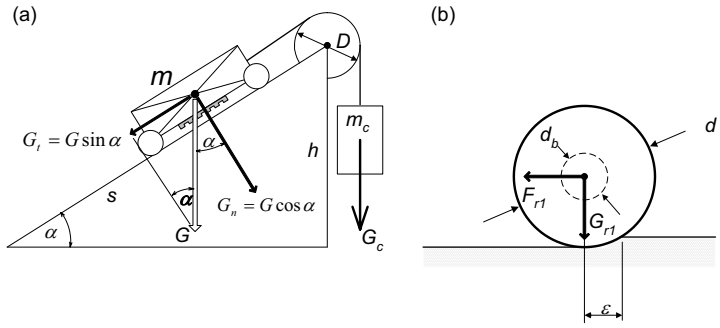

Fig. 1.24. Linear–motor–driven mechanism: (a) slope, (b) sketch for calculating the rolling resistance.

When the moving part runs up the gradient with an acceleration a the acceleration thrust is higher since the term $(m + m_c)a$ is added, i.e.,

$$F_{xpeak} = \frac{1}{\eta}[(m\sin\alpha + \mu m\cos\alpha - m_c)g + (m + m_c)a] \tag{1.47}$$

The thrust according to eqn (1.47) is often called the peak thrust. Similarly, if the car runs up with a deceleration d, the braking force is

$$F_{xb} = \eta[(m \sin\alpha + \mu m \cos\alpha - m_c)g - (m + m_c)a] \tag{1.48}$$

Note that, for the braking mode, the counterbalancing force is $1/\eta(F_{xb}+m_c g)$.

The linear–motor–driven car is furnished with wheels. The rolling force (Fig. 1.24b)

$$F_{r1} = \frac{\epsilon G \cos\alpha}{0.5d}$$

where $G\cos\alpha = G_n = mg\cos\alpha$. Including friction in wheel-axle bearings,

$$F_{r2} = F_{r1} + \frac{0.5 d_b \mu G \cos\alpha}{0.5d} = \frac{\epsilon + 0.5\mu d_b}{0.5d} G\cos\alpha$$

where d_b is the diameter of the bearing journal. An additional resistance due to uneven track and hunting can be added by introducing a coefficient $\beta > 1$. Thus, the total rolling force

$$F_r = k_r G \tag{1.49}$$

where

$$k_r = \beta \frac{(\epsilon + 0.5\mu d_b)\cos\alpha}{0.5d} \tag{1.50}$$

In railway engineering, the coefficient k_r is called the *specific rolling resistance*. For speeds up to 200 km/h and steel wheels on steel rails, $k_r = 0.002$ to 0.012.

Eqn (1.46), in which $m_c = 0$ and $\eta \approx 1$, is known in railway engineering as *traction effort equation* and has the following form:

$$F_x = (k_r + k_g + k_a)G \tag{1.51}$$

The *specific gradient resistance* is

$$k_g = \pm\sin\alpha = \pm\frac{h}{s} \tag{1.52}$$

since the force due to gravity is $G_t = G\sin\alpha$. The "+" sign is for a car moving up the gradient, and the "−" sign is for a car moving down the gradient. Neglecting the inertia of rotating masses of the car, the *specific acceleration resistance* is

$$k_a = \frac{a}{g} \tag{1.53}$$

where a is the linear acceleration or deceleration. For a curvelinear track, the *specific curve resistance* should be taken into account, i.e.,

$$k_c = \frac{0.153S + 0.1b}{R_c} \tag{1.54}$$

where S is the circumference of wheel in meters, b is the mean value of all fixed wheel bases with $b < 3.3S$ in meters, and R_c is the track curve radius in meters. For example, if the wheel radius is $R = 0.46$ m, the wheel base is $b = 3$ m and the track curve radius is $R_c = 5$ km, the circumference of wheel $S = 2\pi R = 2\pi \times 0.46 = 2.89$ m, and the specific curve resistance is $k_c = (0.153 \times 2.89 + 0.1 \times 3.0)/5000 = 0.148 \times 10^{-3}$.

For high-speed trains the air resistance force

$$F_{air} = 0.5C\rho v^2 A \quad \text{N} \tag{1.55}$$

should be added to eqn (1.51). The coefficient $C = 0.2$ for cone- or wedge-shaped nose, $C = 2.1$ for flat-front trains, and $C = 0.75$ for automobiles. The air density is ρ, the speed v is in meter/second and the front surface area A is in square meters. At 20°C and 1 atm, the air density is $\rho = 1.21$ kg/m^3. For example, if $C = 0.2$, $v = 200$ km/h $= 200/3.6 = 55.55$ m/s, and $A = 4 \times 3 = 12$ m^2, the air resistance force is $F_{air} = 0.5 \times 0.2 \times 1.21 \times (55.55)^2 \times 12 = 4480.6$ N. Eqn (1.55) gives too small values of the air resistance force for high-speed maglev trains with wedge shaped front cars.

1.5 Selection of Linear Motors

Given below are examples that show how to calculate the basic parameters of linear motion drives and how to choose a linear electric motor with appropriate ratings. This is a simplified selection of linear motors, and more detailed calculation of parameters, especially the thrust, is recommended (Chapter 3).

When designing a linear motor drive, it is always necessary to consider its benefits in comparison with traditional drives with rotary motors and mechanical gears, or ball screws transferring rotary motion into translatory motion [63]. *The authors take no responsibility for any financial losses resulting from wrong decisions and impractical designs.*

Examples

Example 1.1

A moving part of a machine is driven by a linear motor. The linear speed profile can be approximated by a trapezoidal curve (Fig. 1.22a). The total distance of run $s = 1.8$ m is achieved in $t = 0.5$ s with linear acceleration $a = 4g$ at starting, and linear deceleration $d = 3g$ at braking. Find the steady-state speed v_{const}, acceleration time t_1, acceleration distance s_1, constant speed time t_2, constant speed distance s_2, deceleration time t_3, and deceleration distance s_3.

Solution

According to eqn (1.22),

$$k = \frac{1}{2}\left(\frac{1}{4g} + \frac{1}{3g}\right) = 0.02973 \text{ s}^2/\text{m}$$

The constant speed according to eqn (1.23)

$$v_{const} = \frac{0.5}{2 \times 0.02973} - \sqrt{\left(\frac{0.5}{2 \times 0.02973}\right)^2 - \frac{1.8}{0.02973}} = 5.22 \text{ m/s}$$

$$= 18.8 \text{ km/h}$$

The time of acceleration

$$t_1 = \frac{5.22}{4g} = 0.133 \text{ s}$$

The distance corresponding to acceleration

$$s_1 = \frac{1}{2}5.22 \times 0.133 = 0.347 \text{ m}$$

The time of deceleration

$$t_3 = \frac{5.22}{3g} = 0.177 \text{ s}$$

The distance corresponding to deceleration

$$s_3 = \frac{1}{2}5.22 \times 0.177 = 0.462 \text{ m}$$

The time corresponding to the steady-state speed

$$t_2 = 0.5 - 0.133 - 0.177 = 0.19 \text{ s}$$

The distance corresponding to the steady-state speed

$$s_2 = 5.22 \times 0.19 = 0.991 \text{ m}$$

and

$$s_1 + s_2 + s_3 = 0.347 + 0.991 + 0.462 = 1.8 \text{ m}$$

Example 1.2

The specification data of a mechanism with linear motor shown in Fig. 1.24a are as follows: $m = 500$ kg, $m_c = 225$ kg, $\eta = 0.85$, $\alpha = 30^0$, $\epsilon = 0.00003$ m, $\mu = 0.005$, $d = 0.03$ m, $d_b = 0.01$ m, and $\beta = 1.3$. The car is moving up the slope. Find the thrust of the linear motor for (a) steady state, (b) starting with acceleration $a = 1$ m/s^2, (c) braking with deceleration $d = 0.75$ m/s^2. The mass of the cable, pulley, and gears is neglected.

Solution

The weight of the car

$$G = 500 \times 9.81 = 4905 \text{ N}$$

The specific rolling resistance according to eqn (1.50)

$$k_r = 1.3\frac{0.00003 + 0.5 \times 0.005 \times 0.01}{0.5 \times 0.03}\cos 30^0 = 0.00412$$

The steady-state thrust according to eqn (1.46)

$$F_x = \frac{1}{\eta}\left(\sin\alpha + k_r - \frac{m_c}{m}\right)G = \frac{1}{0.85}\left(\sin 30^0 + 0.00412 - \frac{225}{500}\right) \times 4905$$

$$= 312.3 \text{ N}$$

At starting with acceleration $a = 1$ m/s^2 — eqn (1.47),

$$F_{xpeak} = \frac{1}{0.85}\left[\left(\sin 30^0 + 0.00412 - \frac{225}{500}\right) \times 4905 + (500 + 225) \times 1.0\right]$$

$$= 1165.2 \text{ N}$$

The peak thrust of the linear motor should not be lower than the above value. At braking with deceleration $a = 0.75$ m/s^2 — eqn (1.48),

$$F_{xb} = 0.85\left[\left(\sin 30^0 + 0.00412 - \frac{225}{500}\right) \times 4905 - (500 + 225) \times 0.75\right]$$

$$= -236.6 \text{ N}$$

Example 1.3

A 1.5-kW, 1.5 m/s linear electric motor operates with almost constant speed and with the following thrust profile: 1600 N for $0 \leq t \leq 3$ s, 1200 N for $3 \leq t \leq 10$ s, 700 N for $10 \leq t \leq 26$ s, 500 N for $26 \leq t \leq 38$ s. The overload capacity factor $F_{xmax}/F_{xr} = 2$. Find the thermal utilization coefficient of the motor.

Solution

In accordance with eqn (1.2), the rated thrust produced by the linear motor is

$$F_{xr} = \frac{P_{out}}{v} = \frac{1500}{1.5} = 1000 \text{ N}$$

The linear motor has been properly selected since the maximum load for the given thrust profile 1600 N is less than the maximum thrust determined by the overload capacity factor, i.e.,

$$F_{xmax} = 2F_{xr} = 2 \times 1000 = 2000 \text{ N}$$

The rms thrust based on the given duty cycle

$$F_{xrms} = \sqrt{\frac{\sum F_{xi}^2 t_i}{\sum t_i}} = \sqrt{\frac{1600^2 \times 3 + 1200^2 \times 7 + 700^2 \times 16 + 500^2 \times 12}{3 + 7 + 16 + 12}}$$

$$= 867.54 \text{ Nm}$$

The coefficient of thermal utilization of the motor

$$\frac{F_{xrms}}{F_{xr}} \times 100\% = \frac{867.54}{1000.0} \times 100\% = 86.7\%$$

The linear motor, e.g., IC11-200 (Table 1.2) with continuous thrust 1260 N ($F_{xrms} = 867.54 < 1260$ N) and peak thrust 2000 N can be selected.

Example 1.4

In a factory transportation system, linear–motor–driven containers with steel wheels run on steel rails. Each container is driven by a set of 2 linear motors. The loaded container runs up the gradient and accelerates from $v = 0$ to $v_{const} = 18$ km/h in $t_1 = 5$ s, then it runs with constant speed 18 km/h, and finally it decelerates from $v = 18$ km/h to $v = 0$ in $t_3 = 5$ s. The total time of running is $t = 20$ s. Then containers are unloaded within minimum 10 s, and they run back to the initial position where they are loaded again. The time of

loading is minimum 20 s. The speed and force curves of unloaded containers running down the gradient are the same as those of loaded containers, i.e., acceleration in 5 s to $v_{const} = 18$ k/h, run with constant speed and deceleration in 5 s to $v = 0$. The mass of each container, including the load and linear motor, is $m_c = 1200$ kg, without load $m'_c = 300$ kg. The rise in elevation is $h = 3$ m, and specific rolling resistance is $k_r = 0.0025$. The efficiency of the system can be assumed 100%. Find the length of the track, thrust curve, and *rms* thrust.

Solution

The movement of the container can be approximated by a trapezoidal speed-time curve (Fig. 1.22a). The linear acceleration

$$a = \frac{v_{const} - 0}{t_1 - 0} = \frac{18/3.6}{5} = 1 \text{ m/s}^2$$

The linear deceleration

$$d = \frac{0 - v_{const}}{(t_1 + t_2 + t_3) - (t_1 + t_2)} = \frac{-v_{const}}{t_3} = \frac{-18/3.6}{5} = -1 \text{ m/s}^2$$

where $t = t_1 + t_2 + t_3 = 20$ s is the total time of run. The time of running with constant speed

$$t_2 = t - t_1 - t_3 = 20 - 5 - 5 = 10 \text{ s}$$

The total distance of run is equal to the length of the track. According to eqn (1.20),

$$s = \frac{1}{2}vt_1 + vt_2 + \frac{1}{2}vt_3 = \frac{1}{2}\frac{18}{3.6}5 + \frac{18}{3.6}10 + \frac{1}{2}\frac{18}{3.6}5 = 75 \text{ m}$$

The specific gradient resistance

$$k_g = \pm\frac{h}{s} = \pm\frac{3}{75} = \pm 0.04$$

The specific acceleration and deceleration resistances

$$k_a = \frac{a}{g} = \frac{1.0}{9.81} = 0.102 \qquad k'_a = \frac{d}{g} = \frac{-1.0}{9.81} = -0.102$$

The weight of loaded and empty container

$$G = m_c g = 1200 \times 9.81 = 11772 \text{ N}$$

$$G' = m'_c g = 300 \times 9.81 = 2943 \text{ N}$$

The thrust produced by linear motors when the loaded container moves up the gradient

- the loaded container accelerates ($t_1 = 5$ s)

$$F_{xpeak} = (k_r + k_g + k_a)G = (0.0025 + 0.04 + 0.102) \times 11,772 \approx 1701 \text{ N}$$

  or $1701/2 = 850.5$ N per one linear motor;
- the loaded container runs with constant speed ($t_2 = 10$ s)

$$F_x = (k_r + k_g)G = (0.0025 + 0.04) \times 11,772 = 500.3 \text{ N}$$

  or $500.3/2 \approx 250.2$ N per one linear motor;
- the loaded container decelerates ($t_3 = 5$ s)

$$F_{xb} = (0.0025 + 0.04 - 0.102) \times 11,772 = -700.43 \text{ N}$$

  or each linear motor should be able to produce a braking force $-700.43/2 \approx -350.2$ N during the last 5 s of run.

The thrust produced by linear motors when the unloaded container moves down the gradient

- the unloaded container accelerates (5 s)

$$F'_x = (k_r - k_g + k_a)G' = (0.0025 - 0.04 + 0.102) \times 2943 = 189.8 \text{ N}$$

  or $189.8/2 = 94.9$ N per one linear motor;
- the unloaded container runs with constant speed (10 s)

$$F''_x = (k_r - k_g)G' = (0.0025 - 0.04) \times 2943 = -110.4 \text{ N}$$

  or one linear motor should produce $-110.4/3 = 55.2$ N braking force;
- the unloaded container decelerates (5 s)

$$F'''_x = (0.0025 - 0.04 - 0.102) \times 2943 = -410.55 \text{ N}$$

  or each linear motor should produce a braking force of $-410.55/2 \approx 205.3$ N.

The *rms* thrust developed by two linear motors

$$F_{rms} = \frac{(1701^2 \times 5 + 500.3^2 \times 10 + 700.43^2 \times 5 + 0 + ...}{(5 + 10 + 5 + 10 + 5 + 10 + 5 + 20)^{1/2}}$$

$$\frac{... + 189.8^2 \times 5 + 110.4^2 \times 10 + 410.55^2 \times 5 + 0)^{1/2}}{(5 + 10 + 5 + 10 + 5 + 10 + 5 + 20)^{1/2}} = 542.1 \text{ N}$$

The overload capacity factor

$$\frac{F_{xpeak}}{F_{rms}} = \frac{1701.0}{542.1} \approx 3.14$$

It will probably be difficult to find a linear motor with 3.14 peak-to-rms thrust ratio. If no such linear motor is available, the selected linear motor should develop the peak thrust minimum $1701/2 = 850.5$ N, and its rated thrust can be higher than $542.1/2 \approx 271.1$ N.

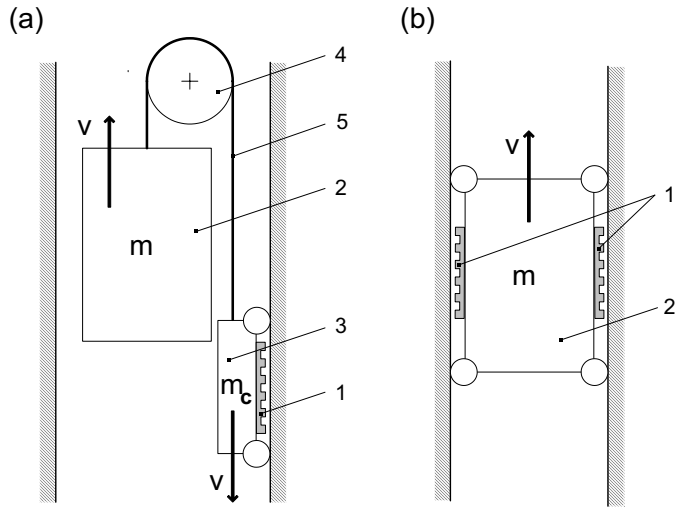

Fig. 1.25. Linear electric motor driven elevators: (a) with a rope; (b) ropeless. 1 — armature of a linear motor, 2 — car (load), 3 — counterweight, 4 — sheave, 5 — rope.

Example 1.5

A linear–motor–driven rope elevator is shown in Fig. 1.25a. The linear motor is built in the counterweight. The mass of the car with load is $m = 819$ kg, the mass of counterweight is $m_c = 1187.5$ kg, the steady-state speed is $v = 1.0$ m/s, the acceleration at starting is $a = 1.0$ m/s^2, and the linear motor efficiency is $\eta = 0.6$. Neglecting the friction, rope mass, and sheave mass, find the steady-state and peak thrust developed by the linear motor and its power consumption at steady state.

Solution

The efficiency of the hoistway is assumed to be $\eta = 100\%$. The thrust at steady state speed when the car is going up can be found on the basis of eqn (1.46) in which $\alpha = 90°$,

$$F_x + m_c g = mg$$

$$F_x = (m - m_c)g = (819 - 1187.5) \times 9.81 = -3615 \text{ N}$$

The car is retarded when going up, and the linear motor should produce a steady-state braking force -3615 N. In the case of drive failure, the elevator car will be moving up, not down, because $m_c > m$.

The peak force at starting — compare eqn (1.47) for $\alpha = 90°$

$$F_{xpeak} = (m - m_c)g + (m + m_c)a = (819 - 1187.5) \times 9.81 + (819 + 1187.5) \times 1.0$$

$$= -1608.5 \text{ N}$$

The ratio $F_{xpeak}/F_x = 1608.5/3615 \approx 0.445$. The linear motor mounted in the counterweight produces smaller braking force at starting than at steady-state speed.

When the car is going down the thrust and the peak thrust are, respectively,

$$F_x = (m_c - m)g = (1187.5 - 819.0) \times 9.81 = 3615 \text{ N}$$

$$F_{xpeak} = (m_c - m)g + (m + m_c)a$$

$$= (1187.5 - 819.0) \times 9.81 + (819.0 + 1187.5) \times 1.0 = 5621.5 \text{ N}$$

The output power of the linear motor at steady-state speed

$$P_{out} = F_x v = 3615.0 \times 1.0 = 3615 \text{ W}$$

The electric power absorbed by the linear motor

$$P_{in} = \frac{P_{out}}{\eta} = \frac{3615}{0.6} = 6025 \text{ W}$$

Example 1.6

Consider a ropeless version of the elevator (Fig. 1.25b). The rope sheave and counterweight have been eliminated, and the linear motor built in the counterweight has been replaced by car-mounted linear motors. Assuming the mass of the loaded car $m = 4583$ kg, $a = 1.1$ m/s^2, $v = 10.0$ m/s, linear motor efficiency $\eta = 0.97$ and two linear motors per car, find the output and input power of linear motors.

Solution

The efficiency of hoistway is assumed to be $\eta = 100\%$. When the car is going up, the requested steady-state thrust is

$$F_x = mg = 4583.0 \times 9.81 = 44,960.0 \text{ N}$$

The requested peak thrust

$$F_{xpeak} = m(g + a) = 4583.0(9.81 + 1.1) \approx 50,000.0 \text{ N}$$

The ratio $F_{xpeak}/F_x = 50,000/44,960 = 1.112$. The steady-state output power of linear motors

$$P_{out} = F_x v = 44,960.0 \times 10.0 = 449,600.0\text{W}$$

or $449,600.0/2 = 224,800.0$ W per one linear motor. It is recommended that two linear motors rated at minimum 225 kW each be chosen, and steady-state thrust $44.96/2 \approx 22.5$ kN at 10.0 m/s and peak thrust $50.0/2 = 25.0$ kN be developed.

When the car is going down, the steady-state breaking force is

$$F_{xb} = -mg = -4583.0 \times 9.81 = -44,960.0 \text{ N}$$

and the transient braking force is smaller,

$$F'_{xb} = -mg + ma = -4583.0 \times 9.81 = 4583.0 \times 1.1 = -39,518.8 \text{ N}$$

The following power can be recovered when regenerative braking is applied:

$$P_b = \eta F_{xb} v = 0.97 \times \mid 44,960.0 \mid \times 10.0 = 436,112.0 \text{ W}$$

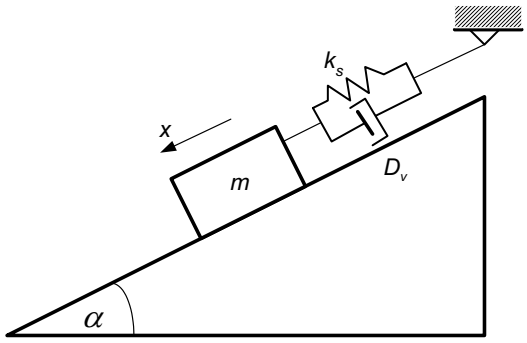

Fig. 1.26. Mass suspended from a linear spring.

Example 1.7

Mass m suspended from a linear spring with spring constant k_s slides on a plane with viscous friction D_v (Fig. 1.26). Find the equation of motion of the mass.

The generalized coordinate is $\xi = x$. The number of degrees of freedom DOF $= 3 - 2 = 1$. The constraint equation $y = z = 0$.

Solution

To solve this problem, Euler–Lagrange equation (1.43) for nonconservative systems will be used.

First method: $E_k \neq 0$, $E_p = 0$, $Q_k \neq 0$

Kinetic energy

$$E_k = \frac{1}{2} m \dot{x}^2$$

Rayleigh dissipation function according to eqn (1.44)

$$Ra = \frac{1}{2} D_v \dot{x}^2$$

External force

$$Q = mg \sin(\alpha) - k_s x$$

Lagrangian

$$\mathcal{L} = E_k - E_p = \frac{1}{2} m \dot{x}^2 - 0 = \frac{1}{2} m \dot{x}^2$$

Derivatives in Euler–Lagrange equation (1.43)

$$\frac{\partial \mathcal{L}}{\partial \dot{x}} = m\dot{x}; \qquad \frac{d}{dt}\left(\frac{\partial \mathcal{L}}{\partial \dot{x}}\right) = m\ddot{x}; \qquad \frac{\partial \mathcal{L}}{\partial x} = 0; \qquad \frac{\partial Ra}{\partial \dot{x}} = D_v \dot{x}$$

Euler–Lagrange equation (1.43) gives the following equation of motion (mechanical balance),

$$m\ddot{x} + D_v \dot{x} + k_s x = mg \sin(\alpha)$$

or

$$m\frac{d^2x}{dt^2} + D_v \frac{dx}{dt} + k_s x = mg \sin(\alpha)$$

Second method: $E_k \neq 0$, $E_p \neq 0$, $Q_k = 0$

Kinetic energy and Rayleigh dissipation function are the same as in the first case. Potential energy

$$E_p = \frac{1}{2}k_s x^2 - mgx\sin(\alpha)$$

Lagrangian

$$\mathcal{L} = E_k - E_p = \frac{1}{2}m\dot{x}^2 + mgx\sin(\alpha) - \frac{1}{2}k_s x^2$$

Derivatives

$$\frac{\partial \mathcal{L}}{\partial \dot{x}} = m\dot{x}; \qquad \frac{d}{dt}\left(\frac{\partial \mathcal{L}}{\partial \dot{x}}\right) = m\ddot{\xi}; \qquad \frac{\partial \mathcal{L}}{\partial x} = mg\sin(\alpha) - k_s x$$

Euler–Lagrange differential equation

$$m\ddot{x} + D_v\dot{x} + k_s x = mg\sin\alpha$$

Both methods give the same results.